JACC: CARDIOVASCULAR IMAGING VOL. 6, NO. 2, 2013

ISSN 1936-878X/$36.00
PUBLISHED BY ELSEVIER INC. http://dx.doi.org/10.1016/j.jcmg.2012.08.016

Mitral Apparatus Assessment by Delayed Enhancement CMR

Relative Impact of Infarct Distribution on Mitral Regurgitation

Jason S. Chinitz, MD,* Debbie Chen, BA,* Parag Goyal, MD,* Sean Wilson, MD,* Fahmida Islam, BA,* Thanh Nguyen, PhD,† Yi Wang, PhD,† Sandra Hurtado-Rua, PhD,‡ Lauren Simprini, MD,§ Matthew Cham, MD,‖ Robert A. Levine, MD,¶ Richard B. Devereux, MD,* Jonathan W. Weinsaft, MD*†

New York, New York; and Boston, Massachusetts

OBJECTIVES This study sought to assess patterns and functional consequences of mitral apparatus infarction after acute myocardial infarction (AMI).

BACKGROUND The mitral apparatus contains 2 myocardial components: papillary muscles and the adjacent left ventricular (LV) wall. Delayed-enhancement cardiac magnetic resonance (DE-CMR) enables in vivo study of inter-relationships and potential contributions of LV wall and papillary muscle infarction (PMI) to mitral regurgitation (MR).

METHODS Multimodality imaging was performed: CMR was used to assess mitral geometry and infarct pattern, including 3D DE-CMR for PMI. Echocardiography was used to measure MR. Imaging occurred 27 ± 8 days after AMI (CMR, echocardiography within 1 day).

RESULTS A total of 153 patients with first AMI were studied; PMI was present in 30% (n = 46 [72% posteromedial, 39% anterolateral]). When stratified by angiographic culprit vessel, PMI occurred in 65% of patients with left circumflex, 48% with right coronary, and only 14% of patients with left anterior descending infarctions ($p < 0.001$). Patients with PMI had more advanced remodeling as measured by LV size and mitral annular diameter ($p < 0.05$). Increased extent of PMI was accompanied by a stepwise increase in mean infarct transmurality within regional LV segments underlying each papillary muscle ($p < 0.001$). Prevalence of lateral wall infarction was 3-fold higher among patients with PMI compared to patients without PMI (65% vs. 22%, $p < 0.001$). Infarct distribution also impacted MR, with greater MR among patients with lateral wall infarction ($p = 0.002$). Conversely, MR severity did not differ on the basis of presence ($p = 0.19$) or extent ($p = 0.12$) of PMI, or by angiographic culprit vessel. In multivariable analysis, lateral wall infarct size (odds ratio 1.20/% LV myocardium [95% confidence interval: 1.05 to 1.39], $p = 0.01$) was independently associated with substantial (moderate or greater) MR even after controlling for mitral annular (odds ratio 1.22/mm [1.04 to 1.43], $p = 0.01$), and LV end-diastolic diameter (odds ratio 1.11/mm [0.99 to 1.23], $p = 0.056$).

CONCLUSIONS Papillary muscle infarction is common after AMI, affecting nearly one-third of patients. Extent of PMI parallels adjacent LV wall injury, with lateral infarction—rather than PMI—associated with increased severity of post-AMI MR. (J Am Coll Cardiol Img 2013;6:220–34) © 2013 by the American College of Cardiology Foundation

From the *Department of Medicine, Greenberg Cardiology Division, Weill Cornell Medical College, New York, New York; †Department of Radiology, Weill Cornell Medical College, New York, New York; ‡Department of Biostatistics, Weill Cornell Medical College, New York, New York; §Cardiology Division, Memorial Sloan Kettering Cancer Center, New York, New York; ‖Radiology, Mount Sinai Medical Center, New York, New York; and the ¶Massachusetts General Hospital, Harvard Medical School, Boston, Massachusetts. This work was supported by Lantheus Medical Imaging, and a Doris Duke Clinical Scientist Development Award (K23 HL102249-01) to Dr. Weinsaft. The authors have reported they have no relationships relevant to the contents of this paper to disclose.

Manuscript received January 11, 2012; revised manuscript received August 17, 2012, accepted August 20, 2012.

Mitral regurgitation (MR) is a serious consequence of acute myocardial infarction (AMI) that confers risk for adverse outcomes, including heart failure and death (1–3). Despite advances in coronary reperfusion, MR remains common after AMI, occurring in as many as 50% of patients (1,4). Moreover, MR can beget MR, as regurgitation itself contributes to chamber dilation, hypertrophy, and systolic dysfunction (5–7). This cascade can further distort both chamber and valve geometry, resulting in progressive MR. While mitral repair/replacement can effectively treat severe MR and medical therapies can prevent adverse remodeling, clinical outcomes can be compromised if therapy is delayed (8–11). Consistent with these clinical observations, animal studies have demonstrated that early treatment of even moderate MR can reduce left ventricular (LV) volumes, attenuate adverse remodeling, and prevent contractile dysfunction (6). Thus, identification of indexes that predict development and progression of post-AMI MR is important for implementation of effective therapeutic interventions.

See page 235

The mitral valve apparatus includes 2 myocardial components: papillary muscles and the adjacent LV wall (12). Both are believed to contribute to mitral valve integrity through direct contractile effects to maintain valve closure as well as secondary effects on valve geometry (12,13). The link between papillary muscle infarction (PMI) and severe MR is well established in the context of papillary rupture (14–16). It is also possible that lesser degrees of papillary necrosis can produce lesser MR that increases with time. However, PMI can occur without rupture, a phenomenon originally reported in experimental as well as autopsy studies (17–19), and was recently shown in vivo using delayed-enhancement (DE) cardiac magnetic resonance (CMR), which enables high-resolution imaging of both PMI and LV wall infarcts in a manner that closely agrees with pathology-evidenced myocyte necrosis (20–22). Both PMI and LV infarct distribution have been studied as isolated predictors of MR. However, results have varied (5,23–26), possibly because their inter-relationship and potential independent contributions to MR have not been examined.

This study examined patterns and consequences of mitral apparatus infarction after AMI. To this end, CMR was performed to assess cardiac function, geometry, and infarct pattern, including high-resolution 3-dimensional (3D) DE-CMR for PMI. Transthoracic echocardiography (echo) was performed for dedicated assessment of MR. The aims were to determine 1) clinical and imaging predictors of post-AMI PMI; and 2) relative impact of PMI and adjacent LV wall infarction on early post-AMI MR.

METHODS

Population. The population consisted of consecutive patients with first ST-segment elevation MI enrolled in a prospective registry of post-AMI remodeling (clinical trial #NCT00539045) between September 2006 and August 2011 at Weill Cornell Medical College. Patients with intrinsic mitral dysfunction (prolapse, rheumatic, prior surgery) were excluded. Imaging was performed within a pre-specified time limit of 6 weeks after AMI. All patients underwent CMR and echo within 1 day.

Comprehensive clinical data were collected, including cardiac risk factors, coronary artery disease history, New York Heart Association functional class, and medication regimen. Coronary angiograms were reviewed for infarct location and coronary dominance. Cardiac enzymes (creatine phosphokinase, myocardial band fraction) were collected for serologic estimation of infarct size. The study was conducted in accordance with the Weill Cornell institutional review board.

Image acquisition. CARDIAC MAGNETIC RESONANCE. CMR was performed using 1.5-T scanners (General Electric, Waukesha, Wisconsin). Examinations consisted of 2 components: 1) cine-CMR for function/morphology; and 2) DE-CMR for infarct quantification. Cine-CMR was performed using a steady-state free precession pulse sequence. Short-axis images were acquired contiguously from the level of the mitral valve annulus through the apex. Long-axis images were acquired in standard 2-, 3-, and 4-chamber orientations. DE-CMR was performed after intravenous gadolinium infusion (0.2 mmol/kg). In all patients, tailored PMI imaging was attempted using a 3D DE-CMR pulse sequence that provides high-resolution imaging (matrix size 256 × 256; typical in-plane resolution 1.4 × 1.4mm, slice thickness 5 mm) acquired during free-breathing by a navigator gating algorithm (27). When 3D DE-CMR was unsuccessful (16%), imaging was limited to breath-

ABBREVIATIONS AND ACRONYMS

AMI = acute myocardial infarction
CI = confidence interval
CMR = cardiac magnetic resonance
DE = delayed-enhanced
Echo = echocardiography
LAD = left anterior descending artery
LCX = left circumflex
LV = left ventricular
MR = mitral regurgitation
OR = odds ratio
PMI = papillary muscle infarction
RCA = right coronary artery
RF = regurgitant fraction
2D = 2-dimensional
3D = 3-dimensional

held 2-dimensional (2D) DE-CMR. For both 2D and 3D DE-CMR, inversion times were adjusted to null viable myocardium and contiguous short-axis images were acquired throughout the LV.

ECHOCARDIOGRAPHY. Transthoracic echo was performed by experienced sonographers using commercially available equipment (General Electric Vivid-7; Philips ie33) with phased-array transducers. Images were acquired using a pre-specified registry protocol, including dedicated MR assessment in accordance with American Society of Echocardiography consensus guidelines (28). Imaging was performed in parasternal, subcostal, and apical 2-, 3-, and 4- chamber orientations. Color Doppler was used to assess presence and severity of MR on the basis of jet area, depth, vena contracta, and directionality. Pulsed-wave Doppler included assessment of MR duration and pulmonary vein flow profile. Two-dimensional imaging was used for related parameters, including mitral valve and annular morphology.

Image interpretation. CARDIAC MAGNETIC RESONANCE. DE-CMR was used to detect PMI. In accordance with established criteria (13), papillary muscles were defined as discrete myocardial structures within the LV cavity that were typically circular in cross-sectional shape and either anterolateral or posteromedial in location. PMI was deemed present if any papillary hyperenhancement was evident on DE-CMR short-axis images. PMI was further categorized by location and extent—partial or complete—stratified using a threshold of >50% papillary myocardium (Fig. 1).

Global LV infarct size (% LV myocardium) was quantified on DE-CMR using the full-width at half-maximum method (22,29). Reproducibility of infarct size quantification, as tested in a subgroup comprising 15% of the study population (n = 23), yielded small intraobserver (Δ = 0.2 ± 1.5% LV myocardium [limits of agreement = −2.7% to +3.1%]) and interobserver differences (Δ = −0.6 ± 1.3% LV myocardium [limits of agreement = −3.3% to +2.0%]). Left ventricular infarct transmurality was scored using a 17-segment model, 5 points per segment scoring system (0 = no hyperenhancement; 1 = 1% to 25%; 2 = 26% to 50%; 3 = 51% to 75%; 4 = 76% to 100%) (30). Relative infarct burden within designated anterior, inferior, and lateral territories (Fig. 2) was calculated as the proportion of segmental scores contained within each territory, multiplied by global LV infarct size.

The CMR scan was also analyzed for conventional indexes of cardiac structure and function. The LV ejection fraction and cavity volumes were

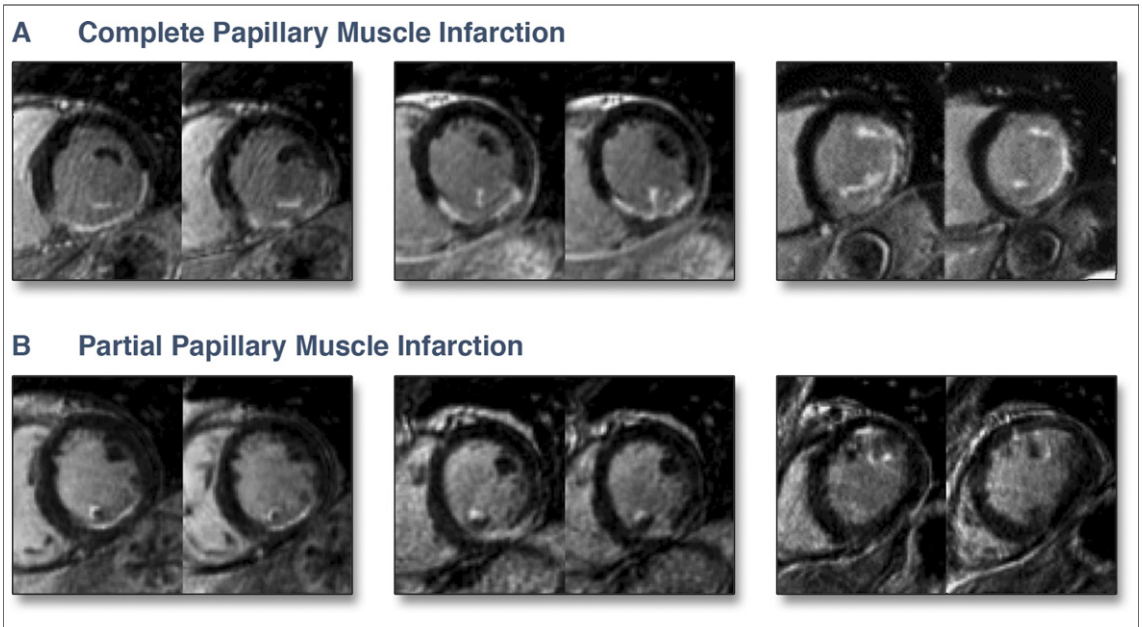

Figure 1. Representative Examples of Complete and Partial PMI

Typical examples of **(A)** complete papillary muscle infarction (PMI) and **(B)** partial PMI detected by delayed-enhancement cardiac magnetic resonance. Each example is composed of 2 short-axis images within the affected papillary muscle. As shown, complete PMI was often associated with transmural infarction of the adjacent left ventricular wall, whereas partial PMI was associated with subendocardial infarction. **Upper right** shows bilateral, complete PMI with transmural infarction of the inferior and lateral walls.

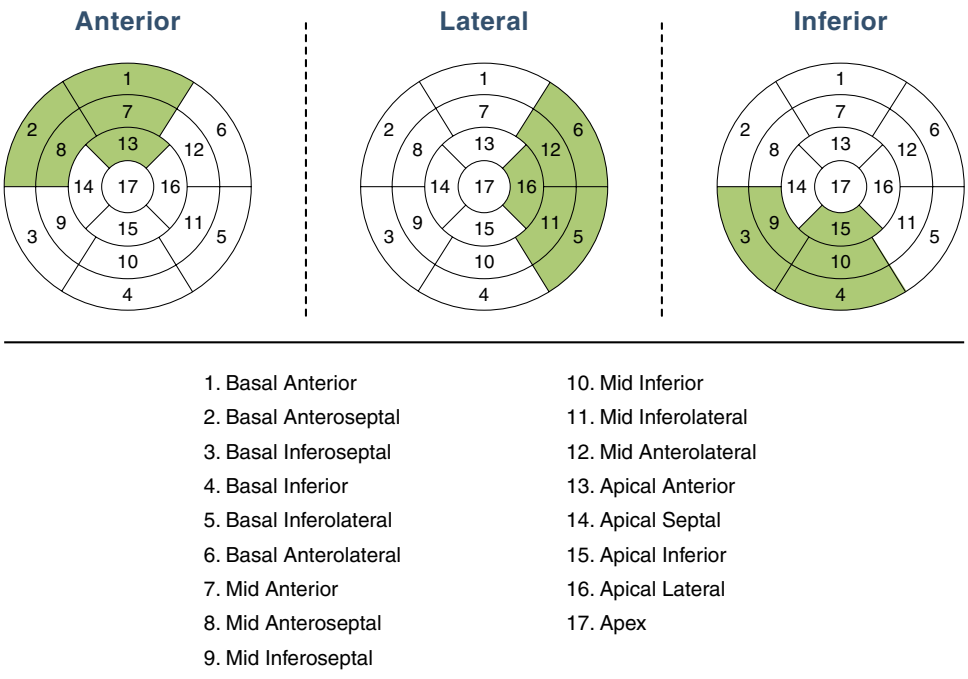

Figure 2. Infarct Distribution

Bullseye plots illustrating segments assigned to each regional infarct category (anterior = anterior/anteroseptal segments; lateral = anterolateral/inferolateral segments; inferior = inferior/inferoseptal segments). Each category was composed of 5 segments (highlighted in **green** in respective bullseye plots), so that total myocardium subtended by each was equivalent.

based on end-diastolic and end-systolic endocardial contours of contiguous short-axis images, with end-diastolic diameter measured in short axis at mid-LV level. Regional LV contractile function was graded using a 17-segment, 5-point scoring system (0 = normal contraction; 1 = mild hypokinesia; 2 = moderate hypokinesia; 3 = severe hypokinesia; 4 = akinesia; 5 = dyskinesia). Left atrial and mitral geometric indexes were measured in accordance with established methodological conventions (26,31). Left atrial area was planimetered in 4-chamber orientation, with volume calculated based on area and chamber length ($8/3\pi \cdot \text{area}^2/\text{length}$) from the posterior left atrium to the mitral annulus (31). Mitral indexes were measured in 3-chamber orientation (26). Mitral annular diameter was measured in a linear plane extending from the respective junctions of anterior and posterior valve leaflets with the atrial wall. Coaptation depth was defined as the distance between leaflet coaptation and the mitral annulus. Tenting area encompassed the area enclosed between the annulus and the mitral valve leaflets. Atrial and mitral annular indexes were measured during ventricular end systole.

ECHOCARDIOGRAPHY. Echocardiography was the reference for MR, which was quantified on the basis of regurgitant fraction (RF). The RF was calculated on the basis of differential stroke volume (SV) as calculated ($\text{VTI} \cdot \pi r^2$) using Doppler and 2D echo indexes acquired at the mitral and aortic valve annuli ($\text{RF} = [\text{SV}_{\text{mitral}} - \text{SV}_{\text{aorta}}] / \text{SV}_{\text{mitral}} \cdot 100\%$). Reproducibility of MR quantification based on regurgitant fraction (32,33) as well as study center expertise for MR assessment (34–36) have been previously reported. Severity of MR was graded using established cutoffs in accordance with American Society of Echocardiography guidelines (mild, RF <30%; moderate, 30% to 39%; moderate-severe, 40% to 49%; and severe, ≥50%) (28). Each respective modality (CMR, echo) was interpreted by an experienced reader blinded to clinical data and other imaging tests.

Statistical methods. Comparisons of continuous variables were made using Student *t* test (expressed as mean ± SD) for 2 group comparisons, with adjunctive use of Levene test to assess for approximate equality of variance between groups. Analysis of variance was used for multiple group comparisons. Categorical variables were compared using Pearson chi-square or,

JACC: CARDIOVASCULAR IMAGING, VOL. 6, NO. 2, 2013
FEBRUARY 2013:220–34

Table 1. Clinical and Conventional Imaging Characteristics in Relation to PMI

	Overall (n = 153)	PMI+ (n = 46)	PMI− (n = 107)	p Value
Clinical				
Age, yrs	57 ± 12	60 ± 13	56 ± 12	0.06
Male	82% (126)	89% (41)	79% (85)	0.15
Atherosclerosis risk factors				
Hypertension	46% (70)	50% (23)	44% (47)	0.49
Hypercholesterolemia	46% (70)	39% (18)	49% (52)	0.28
Diabetes mellitus	25% (38)	26% (12)	24% (26)	0.81
Tobacco use	34% (52)	30% (14)	36% (38)	0.54
Family history	26% (40)	28% (13)	25% (27)	0.70
Prior coronary artery disease				
PCI	5% (7)	9% (4)	3% (3)	0.20
CABG	1% (1)	2% (1)	0% (0)	0.30
NYHA functional class, I/II/III/IV	82% (126)/14% (22)/3% (4)/1% (1)	78% (36)/15% (7)/4% (2)/2% (1)	84% (90)/14% (15)/2% (2)/0% (0)	0.34
Cardiovascular medications				
Beta-blocker	97% (148)	98% (45)	96% (103)	1.00
HMG CoA-reductase inhibitor	94% (144)	96% (44)	94% (100)	0.73
Loop diuretic	5% (7)	4% (2)	5% (5)	1.00
Nitroglycerin	7% (10)	9% (4)	6% (6)	0.49
Aspirin	100% (153)	100% (46)	95% (107)	—
Thienopyridines	95% (145)	91% (42)	96% (103)	0.24
MI treatment strategy				
Thrombolysis	26% (39)	26% (12)	25% (27)	0.91
Percutaneous coronary intervention	75% (114)	74% (34)	75% (80)	0.91
Cardiac magnetic resonance				
Left ventricular function/geometry				
Ejection fraction, %	52.5 ± 11.9	52.3 ± 11.8	52.6 ± 12.0	0.89
Wall motion score	0.8 ± 0.6	0.9 ± 0.6	0.8 ± 0.6	0.45
EDD, cm	5.5 ± 0.5	5.7 ± 0.5	5.5 ± 0.5	**0.02**
EDD, height adjusted	0.03 ± 0.003	0.033 ± 0.003	0.032 ± 0.003	**0.04**
End-diastolic volume, ml	153.1 ± 42.4	163.4 ± 39.2	148.7 ± 43.2	**0.049**
End-diastolic volume index, ml/m^2	77.6 ± 19.0	81.4 ± 17.6	76.0 ± 19.4	0.11
End-systolic volume, ml	75.5 ± 37.4	80.8 ± 37.2	73.2 ± 37.4	0.25
End-systolic volume index, ml/m^2	38.3 ± 18.4	40.3 ± 18.3	37.4 ± 18.5	0.38
Myocardial mass, g	131.1 ± 32.3	136.7 ± 33.5	128.8 ± 31.6	0.17
Myocardial mass index, g/m^2	66.4 ± 14.2	67.8 ± 14.7	65.8 ± 14.0	0.42
Left atrial geometry				
Left atrial diameter, cm	3.6 ± 0.5	3.6 ± 0.6	3.6 ± 0.5	0.91
Left atrial area, cm^2	22.1 ± 4.9	22.2 ± 5.4	22.0 ± 4.7	0.87
Left atrial volume, ml	79.2 ± 27.6	79.6 ± 31.2	79.0 ± 26.0	0.90
Left atrial volume index, ml/m^2	40.4 ± 14.0	39.7 ± 15.0	40.7 ± 13.6	0.67
Mitral annular geometry				
Annulus diameter, cm	2.8 ± 0.4	2.9 ± 0.4	2.8 ± 0.4	**0.046**
Coaptation height, cm	0.6 ± 0.2	0.6 ± 0.2	0.6 ± 0.2	0.82
Tenting area, cm^2	0.9 ± 0.4	0.9 ± 0.4	0.9 ± 0.4	0.64

Values are mean ± SD or % (n). **Boldface** indicates p values <0.05.
CABG = coronary artery bypass graft surgery; EDD = end-diastolic diameter; HMG CoA = 3-hydroxy-3-methylglutaryl-coenzyme A; MI = myocardial infarction; NYHA = New York Heart Association; PMI = papillary muscle infarction.

when <5 outcomes were expected per cell, Fisher exact test. Ordinal variables were compared using Kruskal-Wallis 1-way analysis or the Jonckheere-Tempestra test, with the latter used to test between-group differences in graded MR severity. Logistic regression was used to evaluate multivariable associations between imaging parameters and MR. Two-sided p <0.05 was considered indicative of statistical significance. Calculations were performed using SPSS version 19.0 (SPSS, Chicago, Illinois).

RESULTS

The population consisted of 153 patients with AMI. CMR was performed 27 ± 8 days after AMI (90% >14 days). Echocardiography was performed within 1 day of CMR in all patients (95% within 4 h).

Papillary muscle infarction was present in 30% (n = 46) of patients, among whom 72% had posteromedial involvement and 39% had anterolateral papillary involvement. Concomitant involvement of both papillary muscles was present in 11% (5 of 46) of affected patients. Figure 1 provides representative examples of PMI identified by DE-CMR.

Table 1 details clinical and conventional imaging characteristics of the study population, with stratification on the basis of presence or absence of PMI. Patients with PMI were clinically similar to patients without PMI. Regarding imaging, results demonstrate that PMI was associated with more advanced remodeling based on LV chamber size and mitral annular diameter ($p < 0.05$).

Infarct parameters. Among the total of 46 patients with PMI, nearly half (48%) occurred in the context of RCA culprit-vessel infarction, with the remainder near evenly divided between left anterior descending artery (LAD [28%]) and left circumflex (LCX [24%]) involvement. When stratified by culprit vessel, PMI occurred in 65% (11 of 17) of patients with LCX, 48% (22 of 46) of patients with RCA, and only 14% (13 of 90) of patients with LAD infarcts ($p < 0.001$).

Table 2 examines infarct-related parameters in relation to PMI. As shown, patients with PMI were more likely to have angiography-evidenced LCX culprit vessel involvement (24% vs. 6%, $p = 0.001$) or RCA culprit vessel involvement (48% vs. 22%, $p = 0.002$) than patients without PMI. Regarding infarct distribution on DE-CMR, prevalence of lateral wall infarction was 3-fold higher among patients with, compared to patients without, PMI (65% vs. 22%, $p < 0.001$). Prevalence of inferior wall infarction was 1.6-fold higher among patients with, compared to patients without, PMI (72% vs. 45%, $p = 0.003$).

Regarding infarct size, Table 2 demonstrates that overall % LV infarction by DE-CMR was larger among patients with PMI ($p = 0.03$), with parallel albeit nonsignificant relationships between PMI

Table 2. Infarct Size and Distribution

	PMI			Posteromedial PMI			Anterolateral PMI		
	Present (n = 46)	Absent (n = 107)	p Value	Present (n = 33)*	Absent (n = 120)	p Value	Present (n = 18)*	Absent (n = 135)	p Value
Infarct size									
DE-CMR									
% LV hyperenhancement	16.0 ± 10.9	12.3 ± 8.9	**0.03**	15.4 ± 10.8	12.9 ± 9.2	0.19	20.2 ± 13.3	12.5 ± 8.7	**0.03**
Cardiovascular enzymes									
Creatine phosphokinase	2,590 ± 2,344	2,164 ± 1,836	0.25	2,351 ± 1,782	2,271 ± 2,057	0.85	2,962 ± 3,118	2,201 ± 1,794	0.36
Creatine phosphokinase-MB	243 ± 207	199 ± 188	0.30	256 ± 206	199 ± 189	0.21	191 ± 200	216 ± 195	0.70
Duration of symptoms									
Chest pain interval, h	12.4 ± 9.4	10.2 ± 8.4	0.17	12.4 ± 9.6	10.4 ± 8.5	0.29	13.7 ± 9.6	10.5 ± 8.6	0.15
Infarct distribution									
DE-CMR									
Anterior wall	35% (16)	70% (75)	**<0.001**	12% (4)	73% (87)	**<0.001**	78% (14)	57% (77)	0.09
Lateral wall	65% (30)	22% (23)	**<0.001**	73% (24)	24% (29)	**<0.001**	61% (11)	31% (42)	**0.01**
Inferior wall	72% (33)	45% (48)	**0.003**	91% (30)	43% (51)	**<0.001**	44% (8)	54% (73)	0.44
Anterior + inferior wall	15% (7)	20% (21)	0.52	12% (4)	20% (24)	0.30	28% (5)	17% (23)	0.33
Lateral + anterior wall	17% (8)	12% (13)	0.39	6% (2)	16% (19)	0.25	44% (8)	10% (13)	**0.001**
Lateral + inferior wall	50% (23)	11% (12)	**<0.001**	64% (21)	12% (14)	**<0.001**	39% (7)	21% (28)	0.13
Lateral + anterior + inferior wall	9% (4)	4% (4)	0.24	6% (2)	5% (6)	0.68	22% (4)	3% (4)	**0.007**
Angiography, infarct-related artery									
Left anterior descending	28% (13)	72% (77)	**<0.001**	0% (0)	75% (90)	**<0.001**	72% (13)	57% (77)	0.22
Left circumflex	24% (11)	6% (6)	**0.001**	33% (11)	5% (6)	**<0.001**	22% (4)	10% (3)	0.12
Right coronary	48% (22)	22% (24)	**0.002**	67% (22)	20% (24)	**<0.001**	6% (1)	33% (45)	**0.02**
Anatomically dominant artery†	57% (26)	26% (28)	**<0.001**	79% (26)	23% (28)	**<0.001**	6% (1)	39% (53)	**0.005**

Values are mean ± SD or % (n). **Boldface** indicates p values <0.05. *5 subjects had concomitant posteromedial and anterolateral papillary muscle infarction (PMI). †Either left circumflex or right coronary artery.
CMR = cardiac magnetic resonance; DE = delayed enhancement; LV = left ventricular; MB = myocardial band.

and the enzymatic and clinical indexes of peak creatine phosphokinase and chest pain duration (both p = NS). However, the relation between PMI and infarct size varied according to culprit vessel involvement. Among patients with LAD infarcts, LV infarct size (% myocardium) was similar between patients with and without PMI (18 ± 11% vs. 15 ± 9%, p = 0.32). In contradistinction, Figure 3A illustrates that among patients with either RCA or LCX culprit involvement, PMI was accompanied by a more than 2-fold increase in LV infarct size (p = 0.001 and p = 0.056, respectively).

Although both RCA and LCX infarction increased relative likelihood for PMI, the impact of coronary dominance varied by culprit vessel. Figure 3B first stratifies both RCA and LCX infarcts based on PMI and then stratifies patients with PMI by coronary dominance; among patients with RCA infarcts, PMI exclusively occurred (100%) in the setting of right or codominant coronary anatomy, whereas less than one-half (36%) of patients with PMI and LCX infarcts were left or codominant (p < 0.0001). All RCA infarcts with PMI had posteromedial involvement (n = 22); 50% (11 of 22) had infarcts of the adjacent mid inferolateral wall.

PMI extent and LV infarct transmurality. In more than three-fourths of cases (76%), PMI was partial, as defined by ≤50% papillary hyperenhancement. Figure 4 compares PMI type by anatomic distribution, demonstrating that PMI type (partial vs. complete) did not differ between the anterolateral and posteromedial papillary muscles (p = 0.50).

Figure 5 relates PMI type to both infarct transmurality and severity of contractile dysfunction in the adjoining LV wall. As shown (Fig. 5A), increased extent of PMI was accompanied by a stepwise increase in mean infarct transmurality within adjacent LV segments underlying each papillary muscle (p < 0.001). Similar results were obtained (Fig. 5B) when contractile dysfunction (segmental wall motion score) was used as a surrogate marker for injury (p < 0.001).

Mitral regurgitation. Among the total study population, echo-evidenced MR was mild or less in most cases, with greater severity present in 14% (n = 22) of patients (moderate, n = 7; moderate-severe, n = 12; severe, n = 3). Table 3 reports univariate analyses examining CMR, biomarker, and x-ray angiography parameters in relation to presence or absence of substantial (moderate or greater) MR.

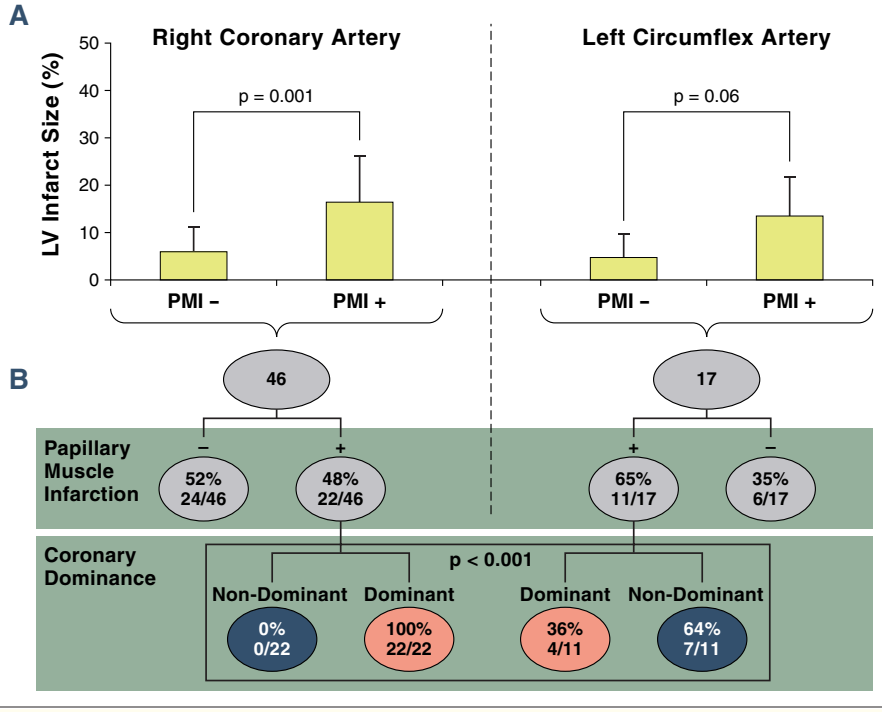

Figure 3. Infarct Size and Coronary Anatomy

(A) Infarct size (mean ± SD) stratified by papillary muscle infarction (PMI) among patients with **(left)** right coronary artery (RCA) and **(right)** left circumflex (LCX) culprit vessels. **(B)** Stratification of RCA and LCX infarcts by presence of PMI **(upper row)** and coronary dominance pattern **(lower row)**. LV = left ventricular.

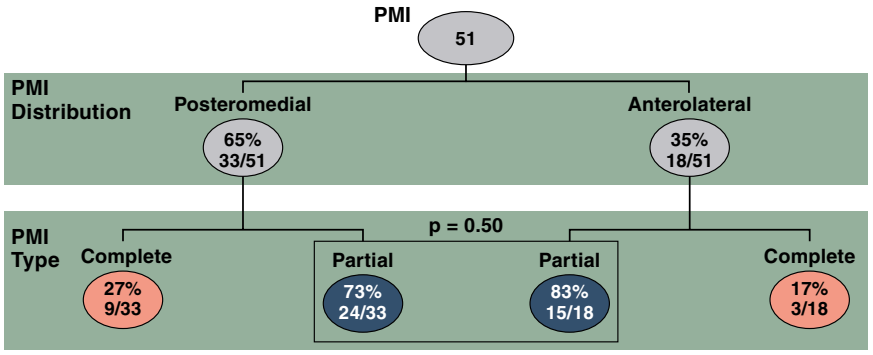

Figure 4. PMI Location and Type

Stratification of papillary muscle infarction (PMI) by location **(upper row)** and type **(lower row)**. Analysis based on total PMI (n = 51) among 46 patients (n = 5 with bilateral PMI).

As shown, patients with moderate or greater MR had worse LV dysfunction and more advanced LV, left atrial, and mitral annular remodeling ($p \leq 0.001$) than patients with lesser or absent MR. Regarding infarct pattern, Table 3 also demonstrates that patients with moderate or greater MR had greater prevalence of lateral wall infarction on DE-CMR ($p < 0.001$), with nonsignificant differences in infarct-related artery distribution potentially attributable to variability in lateral wall coronary vascular supply. Among patients with infarcts that encompassed >1 LV region, only the combination of lateral plus anterior wall infarction was more common among patients with increased MR,

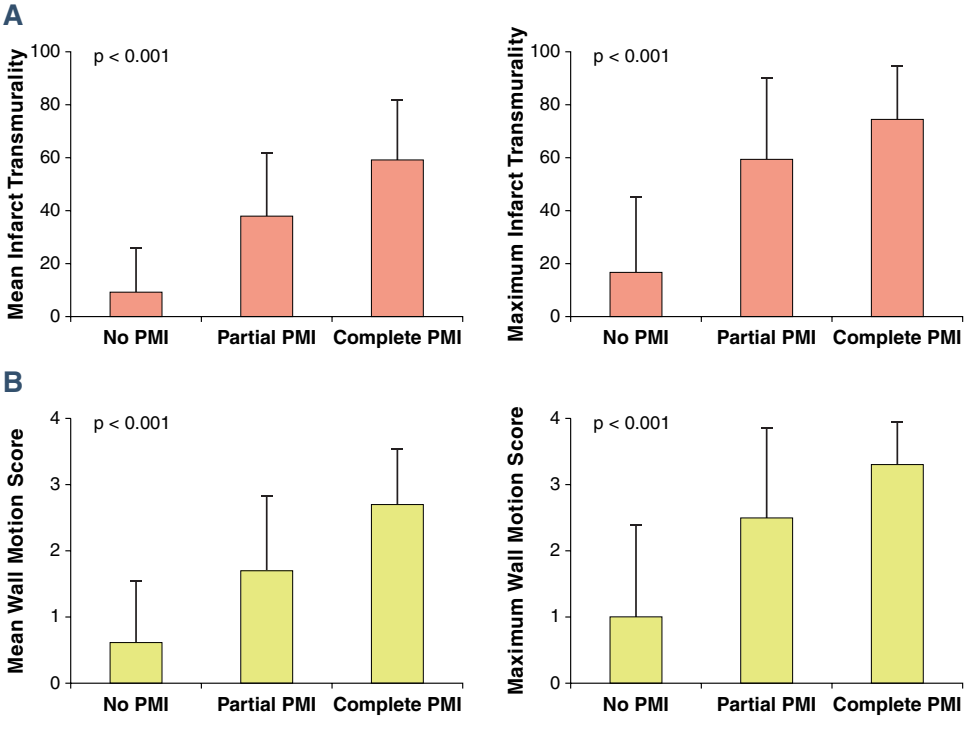

Figure 5. PMI in Relation to Left Ventricular Injury

(A) Infarct transmurality and **(B)** contractile dysfunction stratified by papillary muscle infarction (PMI). Bar graphs based on mean infarct score **(left)** and maximum infarct score **(right)** in left ventricular (LV) segments adjacent to each papillary muscle (posteromedial = mid inferior/inferolateral segments; anterolateral = mid anterior/anterolateral wall segments). Note parallels between PMI extent and severity of injury to adjacent LV segments, whether assessed by infarct transmurality or contractile dysfunction (all $p < 0.001$ for trend).

Table 3. Cardiac Structure, Function, and Infarct Pattern in Relation to Mitral Regurgitation*

	MR+ (n = 22)	MR− (n = 131)	p Value
Mitral annular geometry			
Annulus diameter, cm	3.1 ± 0.4	2.8 ± 0.4	**<0.001**
Coaptation height, cm	0.7 ± 0.2	0.6 ± 0.2	**0.001**
Tenting area, cm^2	1.2 ± 0.5	0.8 ± 0.3	**<0.001**
Left atrial geometry			
Left atrial diameter, cm	4.2 ± 0.6	3.6 ± 0.5	**<0.001**
Left atrial area, cm^2	25.7 ± 5.7	21.6 ± 4.5	**<0.001**
Left atrial volume, ml	98.8 ± 33.7	75.9 ± 25.1	**<0.001**
Left atrial volume index, ml/m^2	49.6 ± 16.5	38.9 ± 13.0	**0.001**
Left ventricular function/geometry			
Ejection fraction, %	42.7 ± 12.2	54.2 ± 11.0	**<0.001**
Wall motion score	1.4 ± 0.8	0.7 ± 0.5	**<0.001**
End-diastolic diameter, cm	6.0 ± 0.6	5.5 ± 0.7	**<0.001**
End-diastolic volume, ml	191.9 ± 46.7	146.6 ± 38.1	**<0.001**
End-diastolic volume index, ml/m^2	97.1 ± 25.7	74.3 ± 15.4	**<0.001**
End-systolic volume, ml	113.8 ± 50.6	69.1 ± 30.5	**0.001**
End-systolic volume index, ml/m^2	57.8 ± 27.2	35.0 ± 14.2	**0.001**
Myocardial mass, g	140.1 ± 32.6	129.6 ± 32.0	0.16
Myocardial mass index, g/m^2	71.1 ± 18.4	65.7 ± 13.3	0.096
Left ventricular infarct pattern			
Infarct size			
% LV hyperenhancement	20.3 ± 12.8	12.3 ± 8.6	**0.009**
Creatine phosphokinase	2730 ± 2009	2215 ± 1995	0.29
Creatine phosphokinase-MB	270 ± 180	205 ± 196	0.28
Infarct distribution (DE-CMR)			
Anterior wall	64% (14)	59% (77)	0.67
Lateral wall	68% (15)	29% (38)	**<0.001**
Inferior wall	59% (13)	52% (68)	0.53
Anterior + inferior wall	27% (6)	17% (22)	0.24
Lateral + anterior wall	41% (9)	9% (12)	**0.001**
Lateral + inferior wall	36% (8)	21% (27)	0.10
Lateral + anterior + inferior wall	14% (3)	4% (5)	0.09
PMI (DE-CMR)	41% (9)	28% (37)	0.23
Infarct-related artery (x-ray angiography)			
Left anterior descending	55% (12)	60% (78)	0.66
Left circumflex	18% (4)	10% (13)	0.21
Right coronary	27% (6)	31% (40)	0.76

Values are mean ± SD or % (n). **Boldface** indicates p values <0.05. *Stratified on the basis of moderate or greater mitral regurgitation threshold.
MR = mitral regurgitation; other abbreviations as in Tables 1 and 2.

consistent with the fact that patients with moderate or greater MR had larger overall LV infarct size (both $p < 0.01$). In multivariable analysis, MR was independently associated with presence of lateral wall infarction (odds ratio [OR] 3.86 [95% confidence interval (CI): 1.40 to 10.69], $p = 0.009$) even after controlling for overall LV infarct size (OR 1.07/% LV hyperenhancement [95% CI: 1.02 to 1.12], $p = 0.01$).

Figure 6 stratifies graded MR severity based on PMI extent and LV infarct distribution on DE-CMR—corresponding data are detailed in tabular form below each bar graph. PMI, categorized by extent of papillary muscle necrosis ($p = 0.12$) or by binary presence/absence ($p = 0.19$), was not associated with increased MR severity. However, LV infarct distribution did impact MR, as evidenced by increased MR severity in association with presence of lateral wall infarction ($p = 0.002$). Of note, lateral wall infarct size was more than 3-fold larger among patients ($n = 5$) with concomitant anterolateral and posteromedial PMI compared to patients with absent or isolated PMI ($p < 0.001$), paralleling a trend toward increased MR severity ($p = 0.09$) in this group.

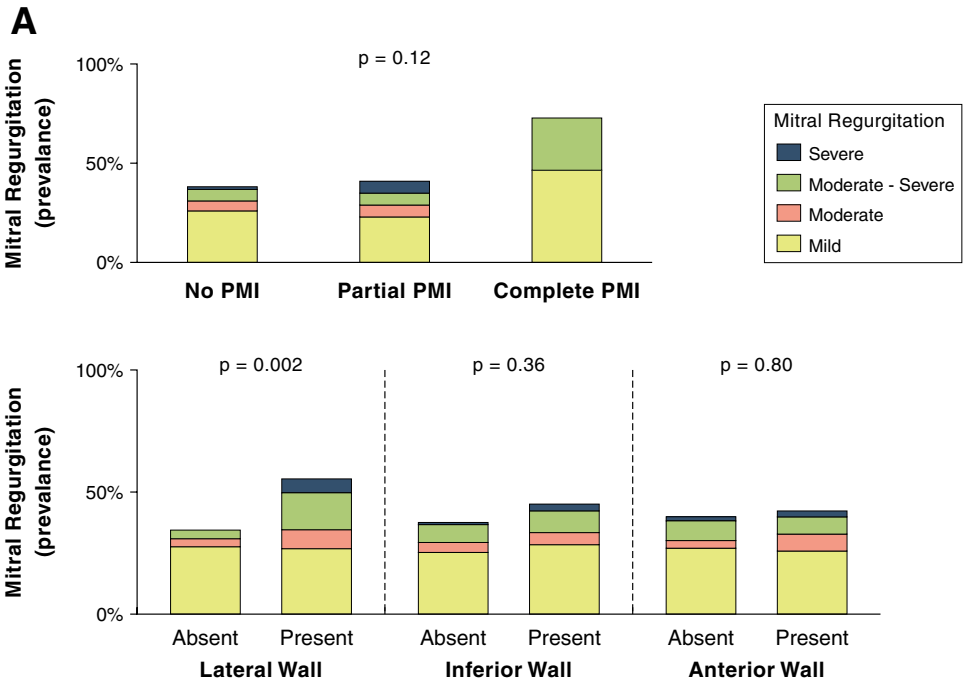

B

			Mitral Regurgitation Severity				
			Absent	**Mild (RF < 30%)**	**Moderate (RF = 30–39%)**	**Moderate-Severe (RF = 39–49%)**	**Severe (RF 50%)**
LV Infarct Distribution	**Lateral**	**Absent**	66% (66)	27% (27)	3% (3)	4% (4)	–
		Present	45% (24)	26% (14)	8% (4)	15% (8)	6% (3)
	Inferior	**Absent**	63% (45)	25% (18)	4% (3)	7% (5)	1% (1)
		Present	56% (45)	28% (23)	5% (4)	9% (7)	3% (2)
	Anterior	**Absent**	60% (37)	27% (17)	3% (2)	8% (5)	2% (1)
		Present	58% (53)	26% (24)	6% (5)	8% (7)	2% (2)
Papillary Muscle Infarction		**Absent**	62% (66)	26% (28)	5% (5)	7% (7)	1% (1)
		Present	60% (21)	23% (8)	6% (2)	6% (2)	6% (2)
		Complete	27% (3)	46% (5)	–	27% (3)	–

Figure 6. Mitral Regurgitation Severity

Graded severity of echocardiography-quantified mitral regurgitation (MR) stratified by **(top)** papillary muscle infarction (PMI) and **(bottom)** left ventricular (LV) infarct distribution. **Dark blue** indicates severe MR; **green** indicates moderate to severe; **orange** indicates moderate; and **yellow** indicates mild. The corresponding table provides a breakdown of MR severity in relation to PMI and LV infarction. RF = regurgitant fraction.

Logistic regression analysis was also used to test the association of infarct distribution with MR after controlling for conventional structural indexes. In the univariate analysis, presence of lateral wall infarction (OR 1.21/% LV myocardium [95% CI: 1.08 to 1.37], p = 0.001) was significantly associated with substantial (moderate or greater) MR, whereas PMI was not (OR 1.76 [95% CI: 0.69 to 4.46], p = 0.24). Multivariate modeling was used to test the independent association of lateral wall infarction with MR after controlling for conventional geometric indexes of mitral annular and LV size. As shown in Table 4, lateral wall infarct size (OR 1.20/% LV myo-

Table 4. Structural Correlates of Mitral Regurgitation

	Univariable Regression		Multivariable Regression *Model χ^2 = 29.37, p <0.001*	
Lateral Wall Infarction	**Odds Ratio (95% CI)**	**p Value**	**Odds Ratio (95% CI)**	**p Value**
Lateral wall infarct size, % myocardium	1.21 (1.08–1.37)	**0.001**	1.20 (1.05–1.39)	**0.01**
Mitral annular diameter, mm	1.29 (1.13–1.48)	**<0.001**	1.22 (1.05–1.45)	**0.009**
LV end-diastolic diameter, mm	1.20 (1.09–1.33)	**<0.001**	1.11 (0.99–1.23)	0.056
PMI, complete or partial	1.76 (0.69–4.46)	0.24		
Complete PMI	2.43 (0.59–9.97)	0.22		
Partial PMI	1.57 (0.59–4.21)	0.37		
	Univariable Regression		**Multivariable Regression** *Model χ^2 = 32.23, p <0.001*	
Lateral Wall Contractility	**Odds Ratio (95% CI)**	**p Value**	**Odds Ratio (95% CI)**	**p Value**
Lateral wall contractile dysfunction (wall motion score)	1.27 (1.13–1.43)	**<0.001**	1.25 (1.08–1.45)	**0.003**
Mitral annular diameter, mm	1.29 (1.13–1.48)	**<0.001**	1.24 (1.05–1.45)	**0.009**
LV end-diastolic diameter, mm	1.20 (1.09–1.33)	**<0.001**	1.07 (0.95–1.21)	0.25
	Univariable Regression		**Multivariable Regression** *Model χ^2 = 23.99, p <0.001*	
Infarct-Related Artery	**Odds Ratio (95% CI)**	**p Value**	**Odds Ratio (95% CI)**	**p Value**
Left circumflex infarction	2.02 (0.59–6.87)	0.26	2.26 (0.59–8.72)	0.24
Mitral annular diameter, mm	1.29 (1.13–1.48)	**<0.001**	1.20 (1.03–1.39)	**0.02**
LV end-diastolic diameter, mm	1.20 (1.09–1.33)	**<0.001**	1.14 (1.03–1.27)	**0.01**

Boldface indicates p values <0.05.
CI = confidence interval; other abbreviations as in Tables 1 and 2.

cardium [95% CI: 1.05 to 1.39], p = 0.01) and mitral annular diameter (OR 1.22/mm [95% CI: 1.05 to 1.45], p = 0.009) were independently associated with MR, with a similar trend for LV chamber diameter (OR 1.11/mm [95% CI: 0.99 to 1.23], p = 0.056). Substitution of lateral wall motion score (OR 1.25 [95% CI: 1.08 to 1.45], p = 0.003) in the model (Table 4) also demonstrated an independent association between lateral wall dysfunction and MR. In contradistinction, use of angiography data did not demonstrate an independent association for LCX (Table 4) culprit involvement. Similar results were obtained when RCA (OR 0.68 [95% CI: 0.21 to 2.18], p = 0.52) or LAD (OR 0.90 [95% CI: 0.32 to 2.51], p = 0.83) culprit involvement was substituted in the model, consistent with overlap in coronary vascular supply to the lateral wall.

DISCUSSION

This study provides new insights regarding prevalence and physiologic consequences of infarction within 2 components of the mitral valve apparatus: papillary muscles and the adjacent LV wall. Key findings are as follows. 1) PMI is common in the current era, affecting nearly one-third (30%) of patients, with relative likelihood greater in the context of LCX or dominant RCA infarcts. 2) PMI typically occurs in the context of increased LV infarct size, as evidenced by a greater than 2-fold increase in infarct size among affected patients with LCX or RCA infarcts. 3) Lateral wall infarction, rather than presence or extent of PMI, is associated with increased MR as measured early after AMI. In multivariate analysis, post-AMI MR is associated with lateral wall infarct size even after controlling for both mitral annular and LV chamber dilation.

Our findings provide new insight into the relation between PMI and MR. Whereas prior studies have reported similar PMI prevalence, results have been discordant regarding PMI as a cause of MR. For example, whereas Tanimoto et al. (25) found no association between PMI and MR, Okayama et al. (26) reported that the 2 were linked. Interestingly, in the latter study, infarction of both papillary muscles was associated with increased MR whereas

single PMI was not. Our results suggest that LV infarct pattern may explain these variable findings. Among our population, only lateral wall infarction was associated with increased MR, and the association between lateral wall infarct size and MR remained significant even after controlling for PMI as well as conventional indexes of LV and mitral geometry. PMI varied in both distribution and extent, with greater magnitude of papillary necrosis associated with increased infarct transmurality within the adjacent LV wall, suggesting that prior reported associations between bilateral PMI and MR may be attributable to increased lateral wall infarct size. Consistent with our results, an association between lateral wall infarction and MR was reported among patients with advanced LV dysfunction (LV ejection fraction <40%) (23), although this prior study did not assess PMI, raising questions as to underlying reasons for MR. To the best of our knowledge, no prior study has examined the inter-relationship of PMI and LV infarct distribution on post-AMI MR.

Our finding that PMI has a negligible impact on MR is consistent with prior animal studies that have examined papillary physiology. Using a canine model in which coronary flow was reduced in a graded fashion, Matsuzaki et al. (37) found that papillary dysfunction alone was insufficient to cause MR, which was instead associated with LV free (lateral) wall hypokinesis and chamber dilation. The importance of lateral wall dysfunction was also demonstrated by Messas et al. (38), who performed targeted LCX occlusion in a sheep model and found that LV inferobasal ischemia produced MR, whereas the addition of papillary ischemia paradoxically decreased MR by reducing leaflet tethering and improving valve coaptation. Regarding mitral geometry, animal studies by Kaul et al. (39) found that MR was associated with incomplete mitral valve closure rather than papillary ischemia. Clinical studies have also supported this concept. Uemura et al. (40), studying 40 patients with prior MI, reported that papillary contractile dysfunction was associated with induction of leaflet tethering and MR attenuation, consistent with our multivariable analysis demonstrating that extent of PMI was not associated with increased MR. Taken together, these prior data support our observation that lateral wall injury and impaired valve coaptation, rather than papillary dysfunction, are key determinants of post-AMI MR.

It is important to recognize that animal studies that have assessed LV injury patterns in vivo have typically relied on LV or papillary contractile dysfunction as surrogates for infarction (37–39), with questions remaining as to the direct impact of myocyte necrosis on mitral valve function. Other studies, which have assessed infarct size directly, have demonstrated the importance of lateral wall infarction using post-mortem analysis, raising uncertainty as to the impact of intrinsic differences between in vivo assessment of mitral geometry/MR and ex-vivo infarct quantification (18,41). To address these issues in a clinical setting, our study employed multimodality imaging for in vivo assessment of infarct size, mitral valve geometry, and MR. The CMR and echo were acquired using a tailored imaging protocol, with both tests performed within a 1-day interval. Results, obtained in a broad cohort of post-AMI patients, offer clinical evidence that both impaired mitral valve geometry (annular diameter) and lateral wall infarct size (% hyperenhancement) are independently associated with post-AMI MR, with a lesser, albeit significant, magnitude of association for LV chamber geometry as measured by end-diastolic diameter.

As DE-CMR provides a highly sensitive tool for assessment of infarct morphology, an additional study goal was to examine the relationship between infarct burden within the papillary muscles and adjacent LV wall. Prior DE-CMR studies, which have also reported increased prevalence of PMI in association with RCA and LCX culprit vessel involvement, have categorized PMI and LV infarct distribution in a binary fashion (25,26). Our study examined graded extent of both papillary and LV wall infarction. Results demonstrate that papillary necrosis occurs in parallel with infarction of the adjacent LV wall, as evidenced by increased LV infarct size in association with greater extent of PMI. Rather than the notion of papillary muscles as end-organ structures particularly susceptible to jeopardized arterial supply, our results support the concept that papillary muscles and LV myocardium are similarly vulnerable to impaired perfusion. Taken together with our findings linking lateral wall infarct size to MR, these data emphasize the importance of prompt coronary reperfusion towards the common goals of preserving LV viability, preventing adverse remodeling, and minimizing MR after AMI.

In addition to CMR and echo, our study included analysis of x-ray angiography for assessment of mitral apparatus perfusion patterns. Results demonstrated that right and left coronary dominance bore a variable impact on PMI. Among patients with RCA infarcts, all with PMI were right (or co-)

dominant whereas for patients with LCX infarcts, less than half (36%) with PMI were left (or co-) dominant ($p < 0.001$). Additionally, we observed a nearly 2-fold higher prevalence of posteromedial (72%) compared to anterolateral (39%) PMI. This difference may be explained by the fact that the posteromedial papillary muscle is typically supplied by a single coronary artery, whereas the anterolateral papillary muscle is more frequently concomitantly perfused by 2 coronary arteries (42). Regarding MR, infarct-related culprit vessel was not independently associated with valvular regurgitation, consistent with the concept of variable arterial supply to the lateral wall.

Study limitations. Several limitations should be recognized. First, despite inclusion of a broad cohort of post-AMI patients, relatively few (14%) had substantial (moderate or greater) MR, consistent with prior population based studies that have examined MR after AMI (43,44). This limited our ability to examine the independent contributions of all structural variables in relation to MR, and may have resulted in some degree of overfitting in our multivariate models, which tested infarct distribution in relation to the 2 established indexes (mitral annular, left ventricular size) conventionally associated with MR. Additionally, as very few affected patients had severe MR, structural variables examined in this study could not be correlated with graded severity of valvular regurgitation. Although MR severity was measured based on regurgitant fraction, it is important to recognize that other well-validated methods for MR assessment, including effective regurgitant orifice area, were not tested. Finally, as MR was assessed within 6 weeks (27 ± 8 days) of AMI, current findings may not apply to longer-term severity of post-AMI MR. Indeed, MR can dynamically change over time and be influenced by LV remodeling as well as medical therapy. Additional research is necessary to examine the independent utility of mitral apparatus infarct pattern—including PMI—for predicting long-term MR severity.

CONCLUSIONS

In summary, this study demonstrates the interrelationship between papillary muscle and regional LV infarction and identifies lateral wall infarction (rather than PMI) as an independent marker for increased MR as measured early after AMI. This is the first in vivo study to directly link regional LV infarct size and, by extension, infarct transmurality to MR. These findings are relevant to the design of therapies to treat MR, and to the tailoring of their application to individual patients. Applied clinically, findings suggest that LV plication therapies (45) might be considered for CAD patients with severe MR and transmural infarction, whereas coronary reperfusion might be more beneficial as a primary strategy for patients with preserved viability in the lateral wall. DE-CMR also has the potential to guide interventional treatments for MR, such as targeted application of papillary repositioning (46,47) based on infarct distribution. More broadly, improved predictive models for MR are clinically important to better identify and promptly treat at-risk patients before development of adverse consequences such as cardiac chamber remodeling, heart failure, and arrhythmias. Further investigation is needed to test long-term predictors of post-AMI MR, as well as the utility of DE-CMR guided strategies to prevent or treat MR and its complications.

Reprint requests and correspondence: Dr. Jonathan W. Weinsaft, Weill Cornell Medical College, Starr-4, 525 East 68th Street, New York, New York 10021. *E-mail: jww2001@med.cornell.edu.*

REFERENCES

1. Amigoni M, Meris A, Thune JJ, et al. Mitral regurgitation in myocardial infarction complicated by heart failure, left ventricular dysfunction, or both: prognostic significance and relation to ventricular size and function. Eur Heart J 2007;28:326–33.
2. Lamas GA, Mitchell GF, Flaker GC, et al, for the Survival and Ventricular Enlargement Investigators. Clinical significance of mitral regurgitation after acute myocardial infarction. Circulation 1997;96:827–33.
3. Grigioni F, Enriquez-Sarano M, Zehr KJ, Bailey KR, Tajik AJ. Ischemic mitral regurgitation: long-term outcome and prognostic implications with quantitative Doppler assessment. Circulation 2001;103:1759–64.
4. Ennezat PV, Darchis J, Lamblin N, et al. Left ventricular remodeling is associated with the severity of mitral regurgitation after inaugural anterior myocardial infarction—optimal timing for echocardiographic imaging. Am Heart J 2008;155:959–65.
5. Neskovic AN, Marinkovic J, Bojic M, Popovic AD. Early predictors of mitral regurgitation after acute myocardial infarction (abstr). Am J Cardiol 1999;84:329–32.
6. Beeri R, Yosefy C, Guerrero JL, et al. Early repair of moderate ischemic mitral regurgitation reverses left ventricular remodeling: a functional and molecular study. Circulation 2007;116 Suppl:I288–93.
7. Beeri R, Yosefy C, Guerrero JL, et al. Mitral regurgitation augments post-myocardial infarction remodeling failure of hypertrophic compensation. J Am Coll Cardiol 2008;51:476–86.

8. Stevens LM, Basmadjian AJ, Bouchard D, et al. Late echocardiographic and clinical outcomes after mitral valve repair for degenerative disease. J Card Surg 2010;25:9–15.
9. Kongsaerepong V, Shiota M, Gillinov AM, et al. Echocardiographic predictors of successful versus unsuccessful mitral valve repair in ischemic mitral regurgitation. Am J Cardiol 2006;98: 504–8.
10. Go AS, Hylek EM, Phillips KA, et al. Prevalence of diagnosed atrial fibrillation in adults: national implications for rhythm management and stroke prevention. The Anticoagulation and Risk Factors in Atrial Fibrillation (ATRIA) study. JAMA 2001;285: 2370–5.
11. Wolf PA, Mitchell JB, Baker CS, Kannel WB, D'Agostino RB. Impact of atrial fibrillation on mortality, stroke, and medical costs. Arch Intern Med 1998;158:229–34.
12. Perloff JK, Roberts WC. The mitral apparatus. Functional anatomy of mitral regurgitation. Circulation 1972; 46:227–39.
13. Roberts WC, Cohen LS. Left ventricular papillary muscles. Description of the normal and a survey of conditions causing them to be abnormal. Circulation 1972;46:138–54.
14. Vlodaver Z, Edwards JE. Rupture of ventricular septum or papillary muscle complicating myocardial infarction. Circulation 1977;55:815–22.
15. Wei JY, Hutchins GM, Bulkley BH. Papillary muscle rupture in fatal acute myocardial infarction: a potentially treatable form of cardiogenic shock. Ann Intern Med 1979;90:149–52.
16. Nishimura RA, Schaff HV, Shub C, Gersh BJ, Edwards WD, Tajik AJ. Papillary muscle rupture complicating acute myocardial infarction: analysis of 17 patients. Am J Cardiol 1983;51: 373–7.
17. Hider CF, Taylor DE, Wade JD. The effect of papillary muscle damage on atrioventricular valve function in the left heart. Q J Exp Physiol Cogn Med Sci 1965;50:15–22.
18. Mittal AK, Langston M Jr., Cohn KE, Selzer A, Kerth WJ. Combined papillary muscle and left ventricular wall dysfunction as a cause of mitral regurgitation. An experimental study. Circulation 1971;44:174–80.
19. Tsakiris AG, Rastelli GC, Amorim Dde S, Titus JL, Wood EH. Effect of experimental papillary muscle damage on mitral valve closure in intact anesthetized dogs. Mayo Clin Proc 1970; 45:275–85.
20. Kim RJ, Fieno DS, Parrish TB, et al. Relationship of MRI delayed contrast enhancement to irreversible injury, infarct age, and contractile function. Circulation 1999;100:1992–2002.
21. Fieno DS, Kim RJ, Chen EL, Lomasney JW, Klocke FJ, Judd RM. Contrast-enhanced magnetic resonance imaging of myocardium at risk: distinction between reversible and irreversible injury throughout infarct healing. J Am Coll Cardiol 2000;36: 1985–91.
22. Amado LC, Gerber BL, Gupta SN, et al. Accurate and objective infarct sizing by contrast-enhanced magnetic resonance imaging in a canine myocardial infarction model. J Am Coll Cardiol 2004;44:2383–9.
23. Srichai MB, Grimm RA, Stillman AE, et al. Ischemic mitral regurgitation: impact of the left ventricle and mitral valve in patients with left ventricular systolic dysfunction. Ann Thorac Surg 2005;80:170–8.
24. D'Ancona G, Biondo D, Mamone G, et al. Ischemic mitral valve regurgitation in patients with depressed ventricular function: cardiac geometrical and myocardial perfusion evaluation with magnetic resonance imaging. Eur J Cardiothorac Surg 2008;34: 964–8.
25. Tanimoto T, Imanishi T, Kitabata H, et al. Prevalence and clinical significance of papillary muscle infarction detected by late gadolinium-enhanced magnetic resonance imaging in patients with ST-segment elevation myocardial infarction. Circulation 2010;122:2281–7.
26. Okayama S, Uemura S, Soeda T, et al. Clinical significance of papillary muscle late enhancement detected via cardiac magnetic resonance imaging in patients with single old myocardial infarction. Int J Cardiol 2011;146: 73–9.
27. Nguyen TD, Spincemaille P, Weinsaft JW, et al. A fast navigator-gated 3D sequence for delayed enhancement MRI of the myocardium: comparison with breathhold 2D imaging. J Magn Reson Imaging 2008;27:802–8.
28. Zoghbi WA, Enriquez-Sarano M, Foster E, et al. Recommendations for evaluation of the severity of native valvular regurgitation with two-dimensional and Doppler echocardiography. J Am Soc Echocardiogr 2003;16:777–802.
29. Flett AS, Hasleton J, Cook C, et al. Evaluation of techniques for the quantification of myocardial scar of differing etiology using cardiac magnetic resonance. J Am Coll Cardiol Img 2011;4:150–6.
30. Sievers B, Elliott MD, Hurwitz LM, et al. Rapid detection of myocardial infarction by subsecond, free-breathing delayed contrast-enhancement cardiovascular magnetic resonance. Circulation 2007;115:236–44.
31. Lang RM, Biereg M, Devereux RM, et al. Recommendations for chamber quantification: a report from the American Society of Echocardiography's Guidelines and Standards Committee and the Chamber Quantification Writing Group. J Am Soc Echocardiogr 2005;18:1440–63.
32. Enriquez-Sarano M, Bailey KR, Seward JB, Tajik AJ, Krohn MJ, Mays JM. Quantitative Doppler assessment of valvular regurgitation. Circulation 1993;87:841–8.
33. Schwammenthal E, Chen C, Benning F, Block M, Breithardt G, Levine RA. Dynamics of mitral regurgitant flow and orifice area. Physiologic application of the proximal flow convergence method: clinical data and experimental testing. Circulation 1994;90: 307–22.
34. Jones EC, Devereux RB, Roman MJ, et al. Prevalence and correlates of mitral regurgitation in a population-based sample (the Strong Heart Study). Am J Cardiol 2001;87:298–304.
35. Kontos J, Papademetriou V, Wachtell K, et al. Impact of valvular regurgitation on left ventricular geometry and function in hypertensive patients with left ventricular hypertrophy: the LIFE study. J Hum Hypertens 2004;18: 431–6.
36. Palmieri V, Bella JN, Arnett DK, et al. Associations of aortic and mitral regurgitation with body composition and myocardial energy expenditure in adults with hypertension: the Hypertension Genetic Epidemiology Network study. Am Heart J 2003;145: 1071–7.
37. Matsuzaki M, Yonezawa F, Toma Y, et al. [Experimental mitral regurgitation in ischemia-induced papillary muscle dysfunction]. J Cardiol 1988;18 Suppl: 121–6, discussion 127.
38. Messas E, Guerrero JL, Handschumacher MD, et al. Paradoxic decrease in ischemic mitral regurgitation with papillary muscle dysfunction: insights from three-dimensional and contrast echocardiography with strain rate measurement. Circulation 2001;104: 1952–7.
39. Kaul S, Spotnitz WD, Glasheen WP, Touchstone DA. Mechanism of ischemic mitral regurgitation. An experimental evaluation. Circulation 1991; 84:2167–80.
40. Uemura T, Otsuji Y, Nakashiki K, et al. Papillary muscle dysfunction attenuates ischemic mitral regurgitation in patients with localized basal inferior left ventricular remodeling: insights from tissue Doppler strain imaging. J Am Coll Cardiol 2005;46:113–9.

41. Gorman JH III, Gorman RC, Plappert T, et al. Infarct size and location determine development of mitral regurgitation in the sheep model. J Thorac Cardiovasc Surg 1998; 115:615–22.
42. Voci P, Bilotta F, Caretta Q, Mercanti C, Marino B. Papillary muscle perfusion pattern. A hypothesis for ischemic papillary muscle dysfunction. Circulation 1995;91:1714–8.
43. Pastorius CA, Henry TD, Harris KM. Long-term outcomes of patients with mitral regurgitation undergoing percutaneous coronary intervention. Am J Cardiol 2007;100:1218–23.
44. Uddin AM, Henry TD, Hodges JS, Haq Z, Pedersen WR, Harris KM. The prognostic role of mitral regurgitation after primary percutaneous coronary intervention for acute ST-elevation myocardial infarction. Catheter Cardiovasc Interv 2011;80:779–86.
45. Liel-Cohen N, Guerrero JL, Otsuji Y, et al. Design of a new surgical approach for ventricular remodeling to relieve ischemic mitral regurgitation: insights from 3-dimensional echocardiography. Circulation 2000;101: 2756–63.
46. Hung J, Guerrero JL, Handschumacher MD, Supple G, Sullivan S, Levine RA. Reverse ventricular remodeling reduces ischemic mitral regurgitation: echo-guided device application in the beating heart. Circulation 2002;106:2594–600.
47. Hung J, Chaput M, Guerrero JL, et al. Persistent reduction of ischemic mitral regurgitation by papillary muscle repositioning: structural stabilization of the papillary muscle-ventricular wall complex. Circulation 2007;116 Suppl: I259–63.

Key Words: mitral regurgitation ■ myocardial infarction ■ papillary muscle infarction.